Fusion Engineering and Design 192 (2023) 113595

Contents lists available at ScienceDirect

Fusion Engineering and Design

journal homepage: www.elsevier.com/locate/fusengdes

Final design of the DTT Toroidal power supply circuit

P. Zito [a,b,*], M. Manganelli [a,b], A. Lampasi [a,b], S. Pipolo [a,b], R. Lopes [c]

[a] National Agency for New Technologies, Energy and Sustainable Economic Development (ENEA), Frascati, Italy
[b] DTT S. c. a r. l., Frascati, Italy
[c] Engineering Department, University of Palermo, Italy

ARTICLE INFO

Keywords:
Toroidal field coil power supply
Quench protection
Fast discharge units
Silicon carbide varistors, Divertor tokamak test (DTT)

ABSTRACT

The Divertor Tokamak Test (DTT) facility is in advanced design and construction phase at the ENEA laboratories in Frascati, Italy, to contribute to the study, the design and assessment of systems for the treatment of heat exhaust. The DTT Toroidal Field (TF) magnet system consists of 18 superconducting coils, fed in series by a single power supply (TFPS), which is a 24-pulses thyristor-based converter with an output DC current up to of 44 kA. In case of a quench in the superconductors, the magnetic energy stored in the coils is extracted by 3 Fast Discharge Units (FDUs) in series with 3 sectors of 6 TF coils. After the respective contracts were awarded, the TFPS and the FDUs are currently in the final design phase which is addressed in this paper. In particular, the analysis is focused on the most innovative aspects of the design, as the use of silicon carbide (SiC) varistors instead of discharge resistors and of a fully electronic and completely redundant high-current switch without any mechanical device.

1. Introduction

The Divertor Tokamak Test (DTT) facility will contribute to the study, design and assessment of systems for the treatment of heat exhaust, aiming to explore different solutions for DEMO and the future commercial reactors. DTT is under construction at the ENEA Research Center in Frascati, Italy [1,2] by a Consortium including the Italian leading technical and scientific institutions, but many contributions are provided by European and worldwide partners.

The DTT Toroidal Field (TF) magnet system consists of 18 identical superconducting coils in Nb_3Sn (cooled down by super critical helium at 4.5 K) due to the required high magnetic fields (up to 11.8 T with 6 T in the plasma center) [3].

The 18 TF coils are connected in series and driven by a single TF power supply (TFPS) [4,5]. The 18 superconducting coils are rated for a current of 42.5 kA [3]. However, since a safety margin of +3.5% is specified for the TFPS, its design output current results to be in practice 44 kA. The TFPS is protected by a crowbar, which allows the free-wheeling circulation of the current in case of overvoltage or other internal faults. In case of a quench event in the superconducting coils, the magnetic energy stored in the coils must be extracted as fast as possible. The quench protection is ensured through 3 Fast Discharge Units (FDUs) in series with the PS and with 3 sectors of 6 TF coils. During the FDU operations, especially at the initial transients, high voltages will appear across each TF coil [6].

The DTT TFPS and the FDUs were procured through international Calls for Tenders launched in 2021. The contract for the TFPS was awarded to the company Jema Energy in March 2022 for a duration of 18 months, while the contract for the FDUs was awarded to the company OCEM Power Electronics in June 2022 for a duration of 48 months. Both systems are currently in the final design phase. This paper is focused on this design, highlighting the innovative aspects, e.g. the use of silicon carbide (SiC) varistors instead of classic discharge resistors and of fully electronic and completely redundant switches without any mechanical device. While classic discharge resistors produce the well-known exponential discharge curves, with varistors the coil current decreases with a quasi-linear behavior. Advantages of the linear or quasi-linear discharge, achieved by active (successive switches) or passive (SiC varistors), versus exponential discharge were widely discussed in [7] and [8].

2. Description of the TFPS circuit

Fig. 1 summarizes the circuit to supply the DTT TF magnet system consisting in 18 superconducting coils [3] connected in series to one TFPS and 3 FDUs. The optimal number of FDUs is a typical trade-off problem between conflicting requirements [9]. In principle, the same discharge characteristics could be obtained by a single FDU for the

* Corresponding author.
E-mail address: pietro.zito@enea.it (P. Zito).

https://doi.org/10.1016/j.fusengdes.2023.113595
Received 10 October 2022; Received in revised form 17 February 2023; Accepted 20 February 2023
Available online 28 February 2023

whole circuit. However, the components of such FDU would reach very high voltages both across terminals and to the ground. Moreover, the actual transient peak voltages, especially inside the superconducting coils, would be much larger with respect to the ideal case [6]. On the other hand, an excessive number of FDUs would complicate the layout due to the increase of superconducting feeders, transition leads and DC busbars [3,9,10]. The use of 3 FDUs in series with 3 sectors of 6 coils was identified as the best trade-off for DTT, as for JT-60SA [11].

The TFPS is a 2-quadrants 24-pulses thyristor-based AC/DC converter able to generate an output DC current up to 44 kA.

As described in Section 4, the FDU is implemented by connecting a dissipative element in series to each coil sector through a high-current switch. In the final implementation, such switch is completely static (based on parallel IGCTs) and fully redundant (two IGCT switches in series).

A relevant aspect in the circuit design consists in the insulation co-ordination. While the rated voltage is relatively low (±100 V), it can be much higher in case of intervention of the FDUs (>5 kV). The presence

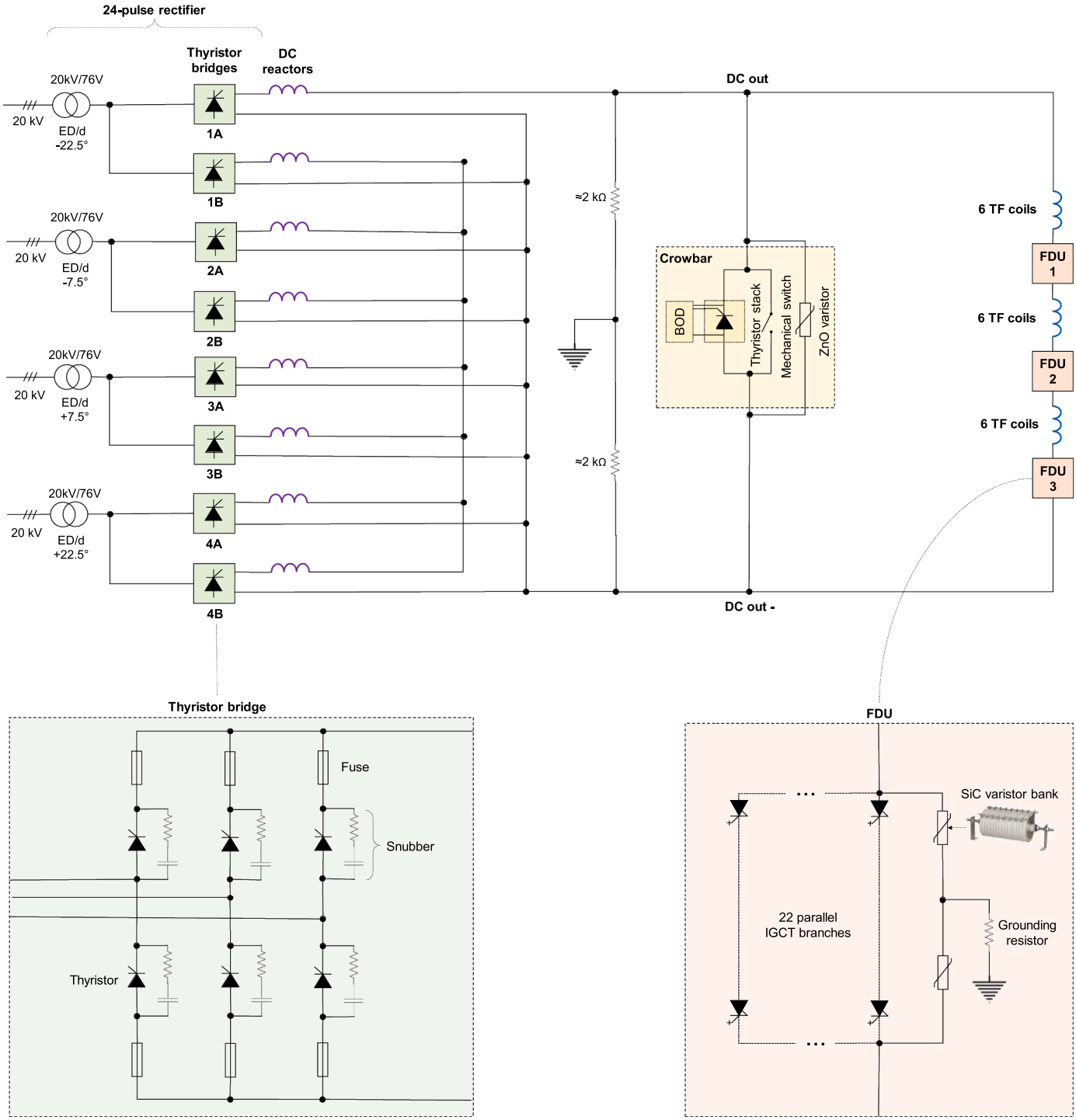

Fig. 1. Simplified electrical scheme of the circuit to supply the 18 TF superconducting coils divided in 3 sectors of 6 coils. The TFPS is a 2-quadrants 24-pulses thyristor-based AC/DC converter with an output DC current up to 44 kA. The (unidirectional) crowbar can be closed to separate the converter and the loads in case of fault. The completely static and fully redundant switches of the 3 FDUs can insert a stack SiC varistor for quench protection.

of the mid-point groundings is only partially considered to keep a safety margin for any situation, also because in the experimental practice the grounding configurations could be modified (for example, by disconnecting a grounding connection). Therefore, the TFPS insulation will be verified at 11.2 kV for 60 s. As there is no a specific standard for FDUs, the IEC Standard 60071 [12] was adopted for similarity to AC circuit breakers. Following this standard, the FDU rated insulation level is 7.2 kV, requiring a test voltage of 20 kV for 60 s (see Section 4.1).

It is interesting to compare some parameters of the DTT TF circuit with those of JT-60SA, another superconducting tokamak in phase of commissioning at Naka, Japan, because they have similar dimensions [11]. The comparisons presented in Table 1 emphasize the main technological challenges in DTT. The parameters in the table and the adopted solutions will be described in the following sections. Moreover, it will be shown that with standard resistors the DTT FDU inrush voltage would be about 6.5 kV.

3. TFPS design

3.1. AC/DC converter and related elements

The TFPS is a 2-quadrants AC/DC converter with the main characteristics summarized in Table 2. Each thyristor bridge (rectifier) in Fig. 1 contains 6 thyristor Dynex DCR3710V14, specifically designed for phase control bridges.

The TFPS input, connected to the DTT medium-voltage (MV) electrical distribution grid at 20-kV level [13], is protected on the MV side by an extractable AC circuit breaker, interlocked with four grounding switches at the secondary terminals of the converter transformers. On the other side, the DC busbars [4,9] are connected through a DC disconnector.

A 24-pulse topology was implemented instead of the 12-pulse topology assumed in [5], even though it could increase costs and space allocation. This is not strictly necessary to comply with the requirement on the output current ripple in Table 2 thanks to the vary large load inductance (≅ 2.2 H). However, the same ripple is also required for the Cold Test Facility where the load is limited to a single TF coil having an inductance of only 48 mH [4]. The use of a 24-pulse topology will also reduce the harmonic pollution towards the MV grid and the AC rated currents and short-circuit currents between the transformers and the thyristor bridges.

Four converter transformers with resin insulation and extended-delta/delta connections produce the angle shifts required by the 24-pulses configuration, also ensuring that, the distribution grid sees the same impedance in any operative condition. In fact, while in the usual configurations combining delta/star and delta/delta transformers the short-circuit voltage drops are different, in the selected configuration the four transformers have very similar characteristics.

In order to avoid branch current unbalance among bridge units due to the phase shift and also to smooth the ripple of the output current, 8 DC reactors are inserted, each at one output terminal of each bridge, as shown in Fig. 1. These reactors are made of aluminum windings and air core, to have a 20 μH inductance, 10 kW total losses, 180 °C thermal insulation class and 100 K temperature rise.

Table 1
Comparison between JT-60SA and DTT TF parameters.

Parameter	JT-60SA	DTT
Equivalent TF inductance	≅ 3.1 H	≅ 2.2 H
TFPS output voltage	±80 V	±100 V
Circuit current	25.7 kA	42.5 kA
Stored magnetic energy	≅ 1 GJ	≅ 2.1 GJ
Discharge time constant	12 s	5 s
FDU inrush voltage	2.8 kV	≅ 5.5 kV

Table 2
Main characteristics of the TFPS.

Parameter	Value
Operations	Steady state
Operation pulses	24
Rated output voltage	±100 V
Rated output current	42.5 kA
Design current with 3.5% margin	44 kA
Current/voltage accuracy	≤1%
Load current ripple	≤0.1%
Insulation test voltage	11.2 kV (for 60 s)

3.2. Crowbar system

The crowbar function is to allow, in case of fault, the freewheeling circulation of the current in the TF circuit, in order to protect it against induced overvoltages. The crowbar is closed at every FDU intervention, while the firing angle of the thyristor bridges is set to 120° The crowbar characteristics are summarized in Fig. 1 and Table 3. The protection is implemented by a hybrid switch consisting of the parallel of a static switch, a mechanical switch and a zinc-oxide (ZnO) varistor [14].

The fast overvoltage protection is assured by the ZnO varistor and by a break-over diode (BOD). The ZnO varistor is able to limit the overvoltage for a short time before the intervention of the static switch. In fact, with respect to the SiC varistors used in the FDUs, a ZnO varistor can absorb much less energy but with a more ideal characteristic [4].

In case of longer overvoltages, the static switch (and, afterwards, the mechanical switch) can be triggered with a high redundancy level either automatically by the internal BOD or by an external command. The static switch is implemented by a stack of 8 thyristors in parallel and it is designed to be able to safely operate even if one thyristor or the mechanical switch is not operating. The mechanical switch takes some tens of milliseconds to close, limiting the conduction time of the thyristors.

3.3. Simulation model and fault analysis

In order to validate the technical choices both in normal operation and in fault conditions, a simulation model of the TF PS was set-up by Jema in PSIM software considering all the subsystems (including thyristor converters, converter transformers, crowbar, DC busbars, FDUs and coils).

Fig. 2 shows a result obtained by the simulation model: the transition from ramp-up to flat-top in normal operation for AC/DC voltages, AC/DC currents and the power factor on the AC side.

An extensive fault analysis was carried out considering the conditions listed in Table 4. From the results summarized in Table 4, the worst fault conditions correspond to the last two considered cases. The related simulation waveforms are reported for these two cases:

1 Figs. 3 and 4 show the waveforms in case of a short-circuit in one thyristor for the global electrical quantities (i.e. DC output current and voltage) and for any bridge rectifier, respectively, assuming that the shoot-through fault occurs in bridge rectifier 1A.
2 Figs. 5 and 6 show the shoot-through fault condition. It should be noted this fault condition requires the intervention of crowbar because of a severe fault condition.

Table 3
Main characteristics of the TF crowbar.

Parameter	Value
Type	Unidirectional
Rated current	44 kA
I^2t	7.2 GA^2s
Number of operations without maintenance	2000
Insulation test voltage	11.2 kV (for 60 s)

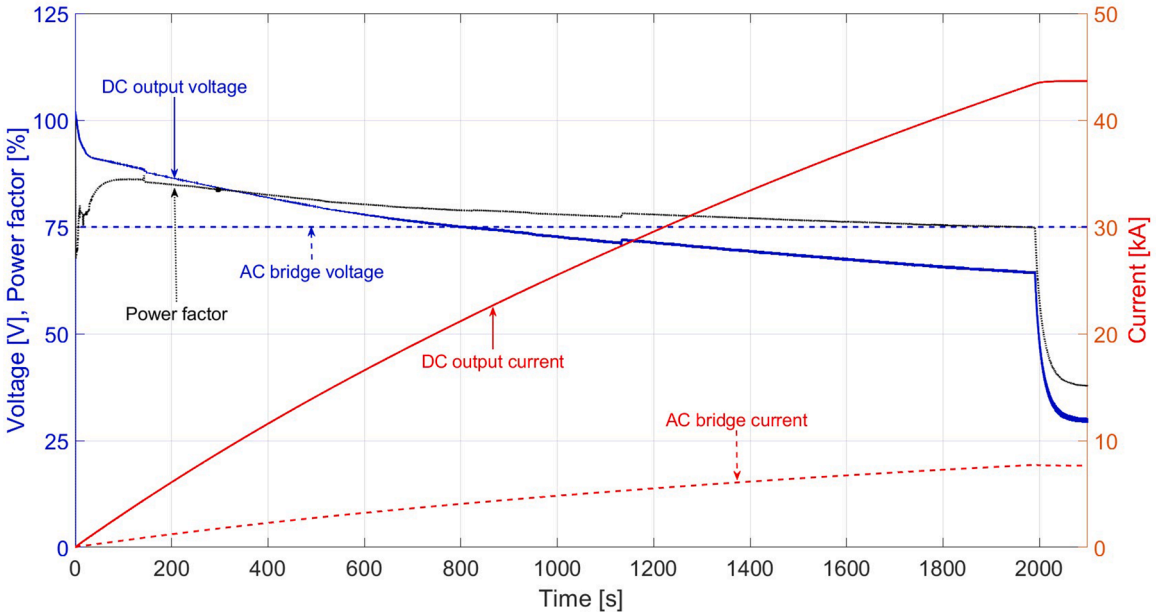

Fig. 2. Input and output electrical parameters of the TFPS obtained by PSIM simulation on the complete load (18 coils) during the transition from ramp-up (lasting 2000s) to flat-top in normal operation.

Table 4
Summary of fault analysis. The transformer peak current is estimated at the low-voltage side.

Fault	DC output current [kA]	DC output voltage [V]	Thyristor peak current [kA]	Transformer peak current [kA]	Thyristor I^2t [MA^2s]
Short-circuit downstream DC reactor at end of ramp-up	43.26	35	8.28	14.56	0.37
Short-circuit downstream DC reactor at beginning of ramp-up	0.73	90	13.16	16.91	1.59
Short-circuit downstream DC reactor at flat-top	43.69	25	7.60	13.71	0.30
Short-circuit upstream DC reactor at end of ramp-up	42.87	35	11.69	17.61	0.61
Short-circuit upstream DC reactor at beginning of ramp-up	1.18	95	13.07	16.72	1.31
Short-circuit upstream DC reactor at flat-top	43.70	25	8.84	14.39	0.32
Thyristor misfiring	43.80	25	5.42	10.66	2.90
Short-circuit in one thyristor	43.99	25	9.29	14.58	6.08
Shoot-through	43.38	25	43.38	0.0	57.89

This analysis was crucial for the correct design of the fuses used to protect the TFPS from short-circuits, installed at the DC output of each thyristor with its own status signaling indication. The fuses were selected and sized to fulfill the two above worst-case faults. Based on these analyses and thyristor rating, the selected fuse model is Mersen URD 2 × 33 TTD 5600, rated for 130 V and 5600 A AC. With this fuse the maximum junction temperature reached by any thyristor in case of fault resulted to be lower than 100 °C that is below the 125 °C allowed for the selected thyristor Dynex DCR3710V14.

4. FDU design

4.1. Function and requirements

The total magnetic energy stored in the superconducting TF coils can exceed 2 GJ [3,6]. This energy is dangerous for the tokamak safety and must be rapidly extracted in case of a quench in the superconductors or for other faults in the systems as in the cryogenic system or in the TFPS itself. The FDUs are designed to safely dissipate this energy by connecting a dump/discharge dissipative element (as a resistor or a varistor) in series to each TF coil sector [9,11], as schematized in Fig. 1.

The requirements for the FDU design derive from the analyses on the superconducting coils [3,6]. It was calculated that a quenched TF coil can sustain a maximum I^2t of 7.2 GA^2s. Since a reliable quench detection requires about 1 s (known as delay time), a part of this I^2t at the maximum current passes through the TF superconducting coil before the opening of the (equivalent) switch, without affecting the dump resistors. The remaining I^2t (the largest part) for the FDU operations is about 5.4 GA^2s and it passes through the elements (resistors or varistors) dissipating the stored magnetic energy. With the reference scheme described in Section 4.2 and assuming a dissipation through traditional linear resistors, it was estimated that the FDU should achieve an exponential discharge with a maximum time constant of 5 s [3,5].

On the other hand, the insertion of a resistance generates a high voltage that is detrimental for the coils, as for the FDU components. The TF coil analysis suggested to require a limitation of the overvoltage to 5.5 kV for each sector of 6 coils.

The maximum rated and fault voltages provide also an indication for the design of the grounding resistors at the mid-point of the FDUs. A deep analysis was performed in [6] moving from the value of 160 Ω. The successive analyses led to a value of about 300 Ω in order to limit the fault current to ground to few amperes. A current sensor with adequate sensitivity was inserted in series to each grounding resistor to detect

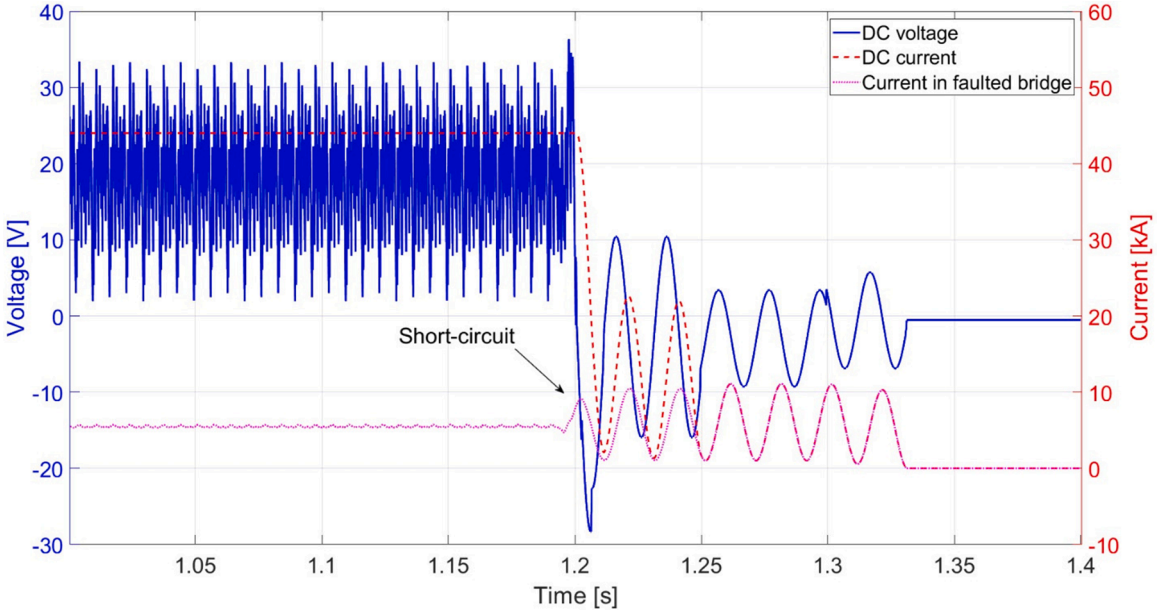

Fig. 3. Effect of a short-circuit in one thyristor.

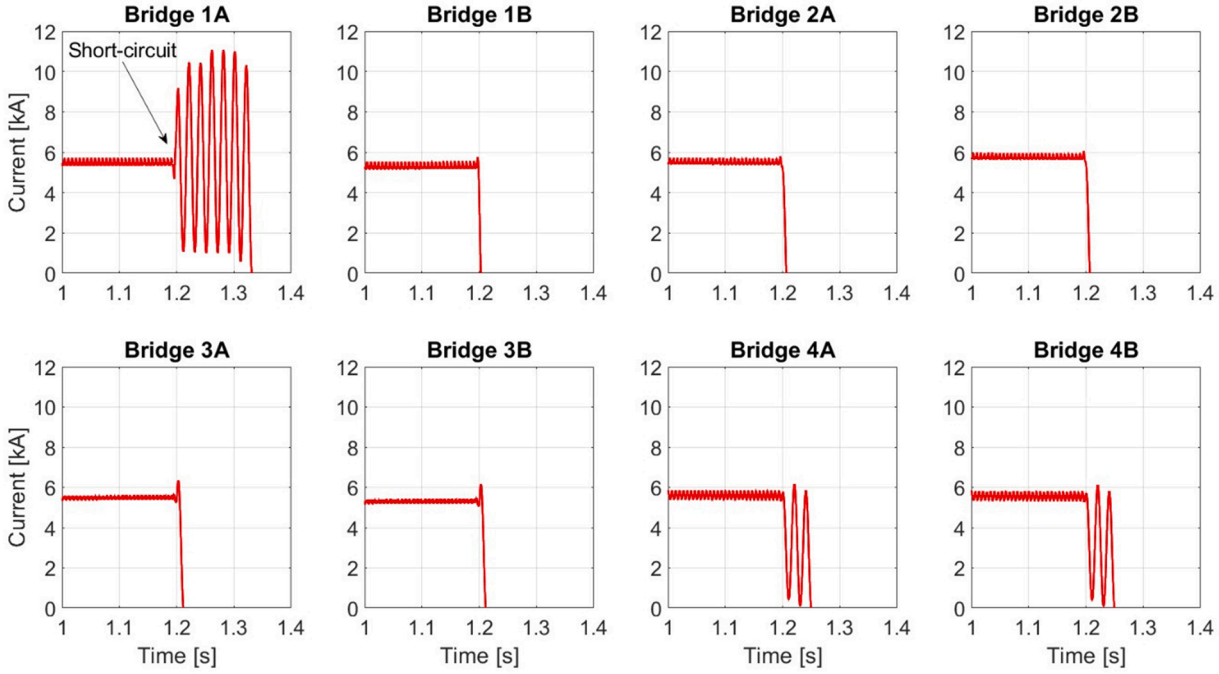

Fig. 4. Effect of a short-circuit in one thyristor in the thyristor bridge 1A on the current of all the 6 bridges.

such fault current.

Whatever is the dissipating element, its temperature evolution during and after fast discharge is a very important parameter. In particular, the minimum interval between two successive discharges is a relevant design specification. The nominal repetition interval in DTT at full power is 1 hour, but the restarting in case of a complete discharge of the TF coils requires a long procedure. Therefore, the repetition interval for the TF FDUs was specified at 3 h. Table 5 summarizes the main FDU requirements resulting from the above discussion.

4.2. Reference scheme

Fig. 7 shows the preliminary reference scheme for the TF FDU, similar to those adopted in [11] and [15], consisting of:

- A mechanical by-pass switch (BPS);
- A static breaker based on IGCTs;
- A dump/discharge resistor (divided in two units by the mid-point grounding);
- A back-up protection made by a pyrobreaker.

The principles of the hybrid switch implemented by the BPS and by the static breaker are extensively described in [15]. With this scheme, in case of a detected quench, two commands are simultaneously sent to open the BPS and to close the static breaker. The static breaker closes immediately, but, since it is characterized by a higher impedance, it

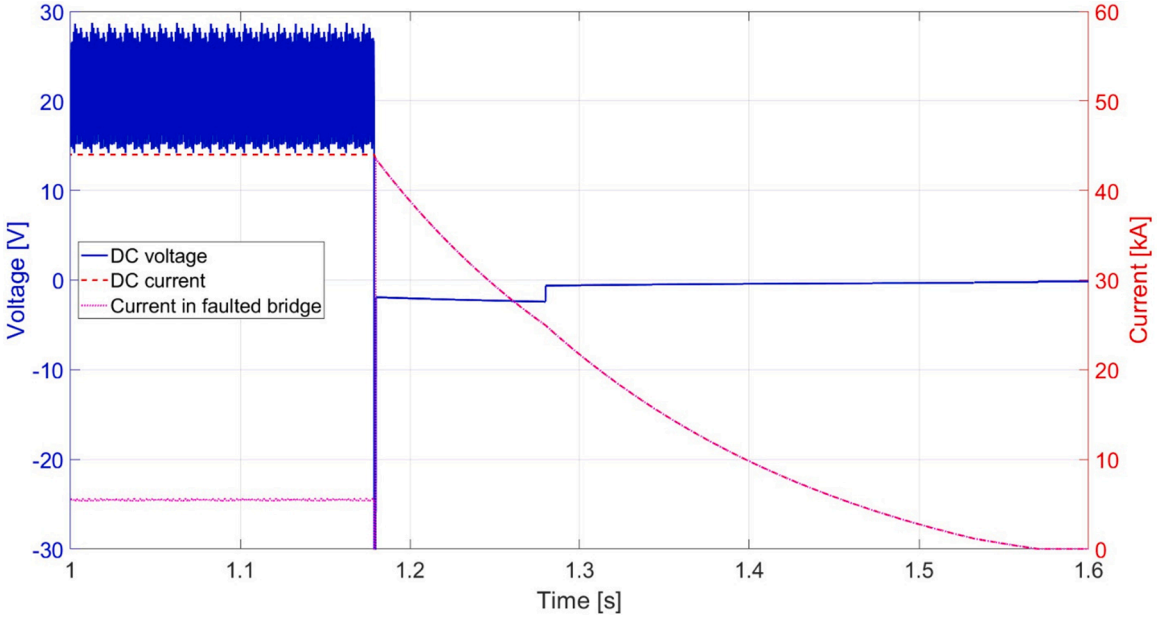

Fig. 5. Effect of the shoot-through fault condition.

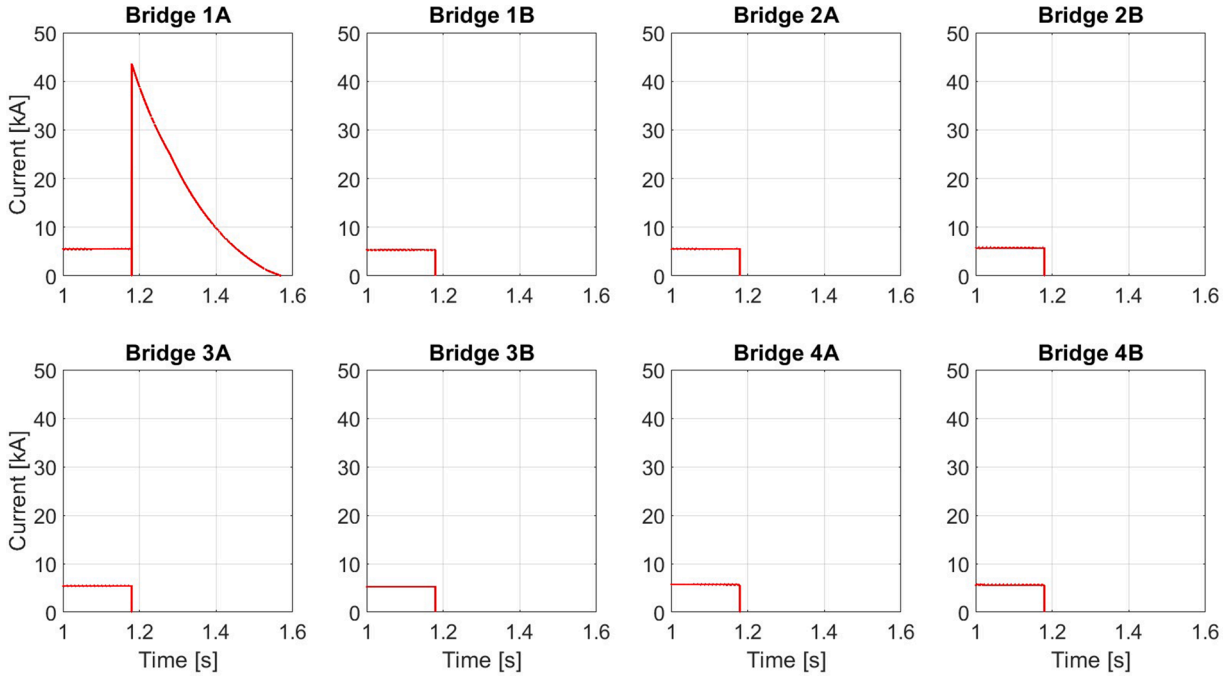

Fig. 6. Effect of the shoot-through fault condition in the thyristor bridge 1A on the current of all the 6 bridges.

cannot conduct current until the BPS is closed. When the BPS contacts start to open, a limited arc is formed producing a voltage able to force a current commutation from the BPS to the static breaker. The static breaker is kept closed until the current commutation is over and the BPS contacts are fully open. Afterwards, the successive opening of the static breaker coincides with the opening of the FDU equivalent switch. It is clear that the equivalent opening time of this hybrid FDU is determined by the full opening time of the BPS, that is in the order of hundreds of milliseconds. Finally, the pyrobreaker is very fast in opening the circuit, but, as it can be triggered only after a reasonable time to be sure that the other devices are not working, it typically takes at least 500 ms to operate [11,16,17].

4.3. *Use of SiC varistors as dissipative elements*

In the final design of the DTT FDUs the standard resistors (in stainless steel) were replaced by properly designed SiC varistors achieving a quasi-linear and faster discharge [8] instead of an exponential current discharge (as commonly implemented in tokamaks [11,18]). In fact, standard resistors, even neglecting the transient effects due to the parasitic elements, would produce a voltage across the switches $\geq$6.5 kV to comply with the discharge time and I^2t specifications in Table 5, then forcing to use two ICGTs in series, that is a much more complicated and unexplored configuration.

The SiC varistors provide more freedom in the optimization of the peak voltage. In order to keep a good safety margin, the peak voltage

Table 5
Main requirements for the TF FDUs.

Parameter	Value
Type	Unidirectional
Operating current	42.5 kA
Maximum inrush voltage of one FDU	5.5 kV
Maximum opening time	500 ms
Opening for static switch	≅1 ms
Equivalent exponential time constant	5 s
Total energy to be dissipated in one FDU	≅0.7 GJ
Specific energy through (I^2t)	7.2 GA^2s
Repetition interval	3 h
Rated insulation level (IEC 60,071 [12])	7.2 kV
Insulation test voltage	20 kV (for 60 s)

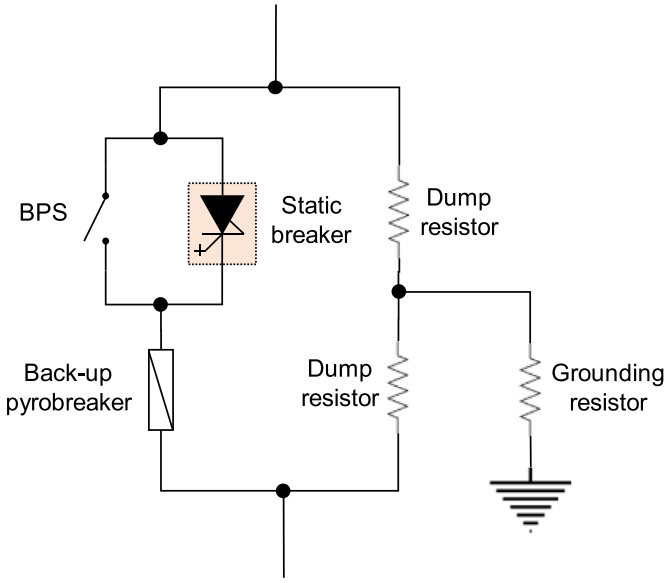

Fig. 7. Preliminary reference scheme of a TF FDU.

was established at about 5.2 kV, that is much less than the minimum 6.5 kV required by the standard resistors. Figs. 8 and 9 compare the FDU current and voltage, respectively, during a discharge, considering the SiC varistors and standard resistors producing the same peak voltage (5.2 kV). Even though the varistor curve in Fig. 8 is less linear than for other cases [8], Fig. 8 exemplifies a general property of varistors: the discharge is much faster with respect to resistors producing the same peak voltage. Similarly, it will be easier also to achieve a $I^2t \leq 7.2\ GA^2s$. Therefore, the adopted technical solution allows a relevant reduction of

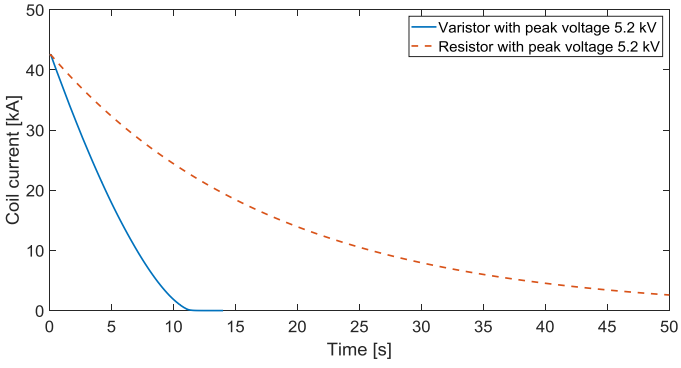

Fig. 8. Comparison between the currents in the TF coils during a fast discharge with SiC varistors and with standard resistors having the same peak voltage (5.2 kV).

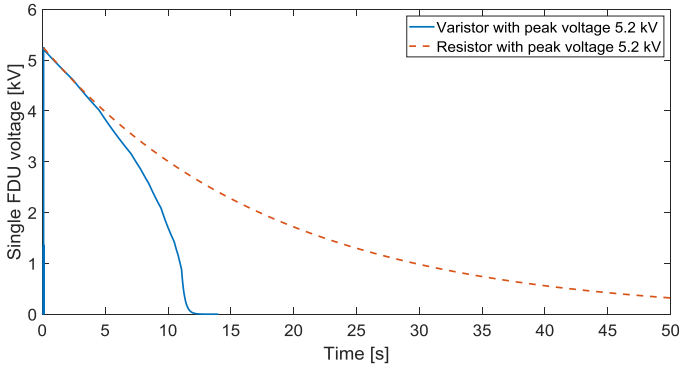

Fig. 9. Comparison between the voltages produced across each FDU with the coil currents in Fig. 8.

the voltage stresses on components and reduced discharge time in a reliable way.

As for standard resistors, the heat generation in varistors during fast discharge is a very important design specification. The varistor bank is sized to recover the ambient temperature in 3 h. Therefore, there is no limitation in the number of successive operations. Of course, the interval could be shorted at lower current or accepting an amount of temperature build-up.

4.4. The adopted solution

Due to the Russia-Ukraine crisis and the subsequent embargo by European Union, the procurement of the pyrobreaker by the Efremov Institute (in Russia) as done in other tokamaks [11,16,17] is not possible. A technical solution to avoid the use of the pyrobreaker is under study also together with OCEM. The priority is to keep the safety of the FDUs by the redundancy of the switches that can be opened. In the reference scheme, the redundancy is achieved by the series of the hybrid switch with the pyrobreaker. Without the pyrobreaker, the same level of redundancy can be preserved in practice only by a different couples of switches, for example by doubling the hybrid switch (mechanical plus static switch), a fully mechanical switch or a fully static IGCT-based switch.

The use of one or two mechanical switches without any static component in parallel was investigated and is still under development for DEMO in collaboration with the EU DEMO Team [9]. However, despite the availability of some interesting prototypes, there are no industrial solutions complaint with the schedules of the DTT project and of the FDU contract. The series of two hybrid switches could work, but would be very expensive, require too much space and be slower in terms of opening time. For both the presented alternatives, it is important to stress that was also hard to find a BPS at 42.5 kA for the hybrid configuration and it would require critical custom tests.

Hence, among the identified solutions, it was chosen to modify the reference scheme in Fig. 7 with the fully-static IGCT-based switch in Fig. 1. In order to achieve a high redundancy, the static switch is doubled not at switch level but at IGCT level: as sketched in Fig. 1, each branch includes two IGCTs in series, each having a separated trigger path. The insertion of fuses in series with every IGCT couple could further improve the reliability of the system, but it is not easy to find on the market reliable fuses for such values of current and energy.

It is important to stress the different function of the IGCTs in the adopted scheme with respect to the reference one in Fig. 7: in the former case the IGCTs conduct for the entire operations (they are switched-off only when the current is diverted to the varistors), whereas in the latter they are used only as support during the commutations [15]. Therefore, the estimated number of IGCTs in parallel is about 3 times with respect to JT-60SA (22 instead of 8). Moreover, by using varistors, the voltage across the FDU is already compliant with the characteristics

of a single IGCT and the use of two IGCTs in series is not forced by the voltage >5.5 kV as it would be for steel resistors, because each IGCT is able to open the rated voltage. The series connection is introduced only to prevent current interruption failures in a IGCT branch.

The fast and simultaneous activation of the two series IGCTs has also the advantage of reducing the energy through the coils and through the varistors. In fact, in the reference scheme in Fig. 7 the worst-case opening time corresponds to the sum of the BPS opening time with the pyrobreaker delay time, that could exceed 500 ms. When the pyrobreaker of one FDU is activated, the other two FDUs that are already opened are dissipating the energy that is not dissipated by the delayed one. Therefore, all the three resistor/varistor banks should be sized to dissipate the energy resulting from only two FDUs opened for 500 ms, that is higher than the energy required by the ideal coil discharge with three FDUs [5].

Another interesting aspect concerns the FDU periodic tests, that are very useful for a protection device. The adopted scheme allows a periodic test of all the IGCTs even at high current. On the other hand, it is not possible to perform tests without flowing a minimal current (no-load test). In the reference scheme, it could be possible to implement a partial test of the BPS at zero-current, but of course there is no way to periodically test the pyrobreaker.

It is interesting to notice that the preliminary layout based on the adopted solution is much more compact that those estimated with the reference scheme, especially if compared with the solution with switched resistor proposed in [7]. Even though there is not a formal reason for that, probably the varistors allow an optimization of the trade-off between the maximum voltage, discharge time and the I^2t specifications [8].

A comparison between the adopted solution and the reference scheme was also performed by a SWOT (Strengths, Weaknesses, Opportunities, Threats) analysis, here synthetically described in Table 6. Advantages of the fully static solution are manifest with respect to the reference scheme. Nevertheless, a pyrobreaker could be inserted in the circuit when the international situation would allow it.

Finally, it must be noted that the main weakness of the new scheme is related to the power losses. In fact, in the reference scheme the IGCTs operate only for less than 1 s, whereas they have a steady-state conduction in the adopted solution. Thus, an adequate water cooling system is necessary to extract to heat form the IGCTs. In order to reduce the power dissipation, customized IGCTs with a specific treatment to reduce the voltage drops were requested to the manufacturer. Thanks to these devices, the resulting power losses will be less than 200 kW per FDU, while the TFPS losses are about 245 kW. In practice, the adopted scheme requires to increase the size of the cooling system already present in DTT.

Table 6
SWOT analysis of the solution adopted for the DTT TF FDUs.

Strengths	Weaknesses
• Faster (less through energy in coils) • Reduced maintenance due to the absence of mechanical parts (BPS and pyrobreaker); • High reliability: • Fully redundant (ICGTs separately fired); • Compact layout; • On-load tests can be often repeated; • Similar costs;	• Higher number of IGCTs; • Higher power losses (due to drop voltages of electronic devices); • Greater water cooling system; • Not possible to perform no-load tests;
Opportunities	Threats
• Use of low voltage drop power devices;	• Vulnerability to electromagnetic interferences and radiations (can be reduced by adequate passive screen)

5. Conclusions

This work was focused on the design of the TFPS and FDUs for the DTT TF circuit. The innovative aspects of the design were pointed out. The TFPS is noticeable for the low DC current ripple and the low harmonic content on AC side due to the 24-pulse converter. A relevant innovation consists in using SiC varistors as dissipative elements in the FDUs, in order to achieve a safer and faster current discharge when required. Another relevant aspect of the FDU design was the exploration of alternatives to the (originally planned) pyrobreaker, leading to a fully static IGCT-based solution.

It is important to stress that other alternative technical solutions were examined and excluded, mainly because not compatible with the times and budget of the DTT FDUs. Regarding these new options, there are no technical solutions already on the market, also long time of R&D activities would be necessary. In any case, any further solution, once available, would be quite more expensive and it would require a greater layout in terms of occupied area and volume. Its higher costs are mainly due to small sales volumes, but this scenario could change in next future. At the moment, it is very difficult to find a company/partner available to develop such equipment, even funding integrally the R&D activities. Nevertheless, these options are being evaluated also in collaboration with the EU DEMO Team.

The present world crisis and increased raw material costs have affected both procurements, causing delays on supplies and the review of the technical choices. Several solutions were implemented in collaboration with the involved companies to limit the delays and also to recover them within the end of contracts. Accordingly, there is a confidence to reach all milestones of contracts on planned times and costs.

Both the TFPS and the first FDU are expected to be installed in 2023 at the Frascati Coil Cold Test Facility in order to start with the tests of the DTT TF superconducting coils at full current. The same TFPS and the FDU could be used also to test the DTT central solenoid (CS) and poloidal field (PF) coils.

Declaration of Competing Interest

The authors declare that they have no known competing financial interests or personal relationships that could have appeared to influence the work reported in this paper.

Data availability

Data will be made available on request.

References

[1] R. Martone, R. Albanese, F. Crisanti, A. Pizzuto, P. Martin, DTT divertor tokamak test facility interim design report, in: ENEA (ISBN 978-88-8286-378-4), April 2019.
[2] R. Ambrosino, DTT - divertor tokamak test facility: a testbed for DEMO, Fusion Eng. Des. 167 (2021), 112330.
[3] A. Di Zenobio, et al., DTT device: conceptual design of superconducting magnet system, Fusion Eng. Des. 146 (Apr 2017) 299–312.
[4] A. Lampasi, et al., Overview of the DTT coil power supplies, Fusion Eng. Des. 188 (March 2023), 113442.
[5] P. Zito, et al., Conceptual design and modeling of the Toroidal Field coils circuit of DTT, in: 20th IEEE Mediterranean Electrotechnical Conference (MELECON), 2020, pp. 617–622.
[6] G. Messina, et al., Transient electrical behavior of the TF superconducting coils of divertor Tokamak test facility during a fast discharge, IEEE TAS 32 (Art) (Jun. 2022), 4901610.
[7] C.R. Lopes, et al., Design optimization for the quench protection of DTT's superconducting Toroidal Field magnets, Fusion Eng. Des. 172 (2021), 112748.
[8] A. Lampasi, Benefits of high-energy varistors in breakdown and fast discharge units, Fusion Eng. Des. 187 (Feb. 2023), 113366.
[9] E. Gaio, et al., Status and challenges for the concept design development of the EU DEMO Plant Electrical System, Fusion Eng. Des. 177 (April 2022), 113052.
[10] A. Cocchi, G. De Marzi, A. Lampasi, R. Romano, Electrothermal design of DC busbars for fusion facilities, Fusion Eng. Des. 170 (September 2021), 112662.
[11] L. Novello, et al., Advancement on the procurement of power supply systems for JT-60SA, in: IEEE 25th Symposium On Fusion Engineering (SOFE), Austin, Texas, USA, May 31-June 4, 2015.

[12] IEC Standard 60071-1:2019, "Insulation co-ordination and system engineering of high voltage electrical power installations above 1,0 kV AC and 1,5 kV DC".
[13] M. Caldora, M.C. Falvo, A. Lampasi, G. Marelli, Preliminary design of the electrical power systems for DTT nuclear fusion plant, Appl. Sci. 11 (12) (2021) 5446.
[14] P. Zito, et al., Design and testing of Crowbar Protection System for the JT-60SA superconducting magnet power supplies, Fusion Eng. Des. 124 (November 2017) 131–136.
[15] A. Lampasi, et al., Final design of the Switching Network Units for the JT-60SA Central Solenoid, Fusion Eng. Des. 89 (2014) 342–348.
[16] M. Manzuk, S. Avanesov, A. Roshal, K. Bestuzhev, A. Nesterenko, S. Volkov, The 70kA pyrobreaker for ITER magnet back-up protection, Fusion Eng. Des. 88 (9–10) (2013) 1537–1540. Issues.
[17] I. Song. D. K. Lee, Upgraded KSTAR Toroidal Field coil quench protection system, IEEE Transact. Plasma Sci. 48 (6) (June 2020) 1666–1669.
[18] K. Wang, Structure optimization of fast discharge resistor system for quench protection system, IEEE Access 7 (2019) 52122–52131.